

Spontaneous contractility-mediated cortical flow generates cell migration in 3-dimensional environments

R.J. Hawkins,¹ R. Poincloux,² O. Bénichou,¹ M. Piel,² P.Chavrier,² and R.Voituriez¹

¹UMR 7600, Université Pierre et Marie Curie/CNRS, 4 Place Jussieu, 75255 Paris Cedex 05 France

²UMR 144, Institut Curie/CNRS, 26 rue d'Ulm 75248 Paris Cedex 05 France

(Dated: April 18, 2022)

We present a generic model of cell motility generated by acto-myosin contraction of the cell cortex. We identify analytically dynamical instabilities of the cortex and show that they trigger spontaneous cortical flows which in turn can induce cell migration in 3-dimensional (3D) environments as well as bleb formation. This contractility-based mechanism, widely independent of actin treadmilling, appears as an alternative to the classical picture of lamellipodial motility on flat substrates. Theoretical predictions are compared to experimental data of tumor cells migrating in 3D matrigel and suggest that this mechanism could be a general mode of cell migration in 3D environments.

PACS numbers:

Beyond its clear interest in the context of cell and molecular biology [1], the study of cell motility and more generally the understanding of simple mechanisms of self-propelled motion is an important challenge for physics and biomimetic technology. Within this context, identifying mechanisms of migration of micro-organisms and in particular living cells has motivated numerous works in the biology and physics communities [2, 3]. Sustained motion at low Reynolds number necessitates a constant energy input, and therefore an active system, that is a system driven out of equilibrium by an internal or an external energy source. The cell cytoskeleton has been long identified as an example of such an active system. It is a network of semi-flexible filaments made up of protein subunits, interacting with other proteins such as motor proteins which use chemical energy of ATP hydrolysis to exert active stresses that deform the network [1].

Two principal out-of-equilibrium processes have been identified as responsible for cell motility: polymerization (treadmilling) of cytoskeleton filaments and contractility of the cytoskeleton, which results from the interaction between actin filaments and motor proteins. Both polymerization induced motion [2, 3] and contractility induced spontaneous flows [4] have now been observed in-vitro, and studied theoretically [5, 6] and numerically [7]. In all models the key ingredients of motion are an energy input to compensate dissipation and sufficient adhesion or friction with a substrate to acquire momentum. The usual picture of cell locomotion, following classical motility experiments realized on 2-dimensional (2D) flat substrates, is then as follows: the cell lamellipodium builds strong adhesion points with the substrate and pushes its membrane forward by polymerizing actin. At the back, the cell body contracts and breaks the adhesion points [1, 8].

However, the geometry of the cell environment in vivo is significantly different from a flat substrate. The effect of geometry – and in particular confinement – has been shown to play a crucial role in cell migration, en-

abling the use of mechanisms widely different from lamellipodial motility [9, 10]. In this context, studying cell motility in 3D environments is a promising and widely unexplored field. In fact, recent observations [11] reveal that MDA-MB-231 breast tumor cells migrate in 3D matrigel with a spherical shape (see Fig. 1) according to a contraction-based mechanism in absence of actin protrusion or lamellipodium formation at the leading edge. Here, inspired by these experiments, we develop a generic model for motility based on the active contraction of the cell's actin cortex caused by the action of myosin. We analytically identify dynamical instabilities of the cortex and demonstrate that spontaneous cortical flows appear. We show that such cortical flows, observed in many contexts of cell polarization and development [12, 13], can also induce cell migration in 3D environments. Theoretical predictions are compared to experimental data of [11], and more generally suggest that this contractility-based mechanism could be a generic mode of migration in 3D environments which strongly differs from the classical picture of lamellipodial motility.

The model is as follows (see Fig. 1). For the sake of simplicity we consider a cell of spherical shape and conserved volume with radius R , and use spherical coordinates (r, θ, ϕ) (qualitatively similar results are expected for other geometries). The cell cortex is a thin shell of acto-myosin gel which polymerizes at the membrane (which defines the outer boundary at $r = R$) with speed v_p , and depolymerizes with a constant rate k_d . Since the actin cortex can vary in thickness, it can be modeled effectively as a 2D shell of a compressible gel with density $\rho(\theta, \phi, t) = \rho_0(1 + \delta\rho(\theta, \phi, t))$. The average density ρ_0 is set by the polymerization speed v_p according to $\rho_0 = av_p/k_d$ where a is the actin monomer concentration which for simplicity we assume is constant. Mass conservation is then given by Eq. (1) below. In a first approximation we write the pressure in the cortex $P = \alpha\delta\rho - \beta\nabla^2\delta\rho$, where α^{-1} is the compressibility of the gel and β the correlation length of density fluctuations,

and denote $\mathbf{v} = (v_\theta, v_\phi)$ the components of the gel velocity. Here, we consider only irrotational flows in the cortex and therefore write $\mathbf{v} = \nabla\psi$. Hereafter the operator ∇ implicitly acts on the angular variables θ, ϕ . We neglect the effects of actin polarization and assume that the gel is in an isotropic phase. The activity of myosin motors then results in a diagonal active stress $\sigma_{\alpha\beta}^a = -\zeta\mu\delta_{\alpha\beta}$ in the gel which, following [14], we assume is proportional to the local concentration of myosin in the cortex $\mu(\theta, \phi, t)$, where ζ is a phenomenological coupling. In the low Reynolds number regime, which is the relevant regime at the cell scale, the force balance given by Eq. (2) is satisfied, where we denote by ξ the friction with the external medium. Here we assume for the sake of simplicity that viscous effects in the gel are much smaller than friction and can be neglected as assumed in [15]. The case of viscosity dominated dynamics, observed in [13], can be studied along the same line and yields qualitatively similar results. In the cell bulk actin filaments are much

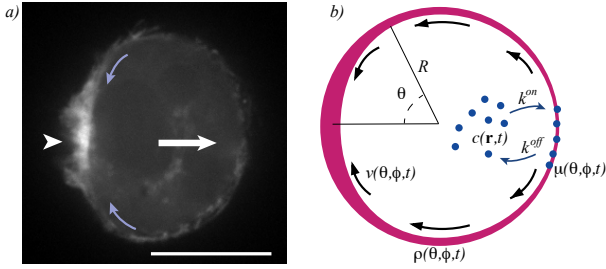


FIG. 1: Cell migration in 3D environments. a) Confocal section of an MDA-MB-231 cell migrating in 3D Matrigel. The cell expresses mCh-Lifeact, a fluorescent probe that labels F-actin [11]. White arrow indicates the direction of movement. Arrowhead points to the accumulation of F-actin at the rear of the cell. Blue arrows indicate the direction of observed cortical flow analyzed in Fig. 4. Scale bar, $10 \mu\text{m}$. b) Cartoon of the model in the first unstable mode $Y_{1,0}$, with the actin cortex in purple. Arrows indicate the velocity of the gel.

more diluted than in the cortex and assumed to be in an isotropic phase, so that myosin, whose bulk concentration is denoted by $c(\mathbf{r}, t)$, diffuses with diffusion constant D_c (see Eq. (3) where Δ denotes the 3D Laplacian). The myosin motors can attach to the cortex at rate k^{on} , where they are transported with the flow of the actin cortex itself and diffuse with diffusion constant D_μ , and can fall off from the cortex with rate k^{off} . Eq. (4) describes the conservation of myosin at the cortex/cytoplasm interface, and Eq. (5) in the cortex. Finally, the non linear dynamical equations for the system are written:

$$\partial_t \delta\rho + \nabla \cdot ((1 + \delta\rho)\nabla\psi) = -k_d \delta\rho \quad (1)$$

$$\nabla \cdot (-\zeta\mu - \alpha\delta\rho + \beta\nabla^2\delta\rho) = \xi\nabla\psi \quad (2)$$

$$\partial_t c = D_c \Delta c \quad (3)$$

$$-D_c \partial_r c|_{r=R} = k^{\text{on}} c(R) - k^{\text{off}} \mu \quad (4)$$

$$\partial_t \mu + \nabla \cdot (\mu\nabla\psi) = k^{\text{on}} c(R) - k^{\text{off}} \mu + D_\mu \nabla^2 \mu. \quad (5)$$

The homogeneous static solution of Eq. (1-5) is trivially given by $\psi = \delta\rho = 0$, $\mu = \mu_0$ and $c = k^{\text{off}}\mu_0/k^{\text{on}}$. In this case there is no actin flow in the cortex and the cell is at rest. To determine the linear stability of this homogeneous state we consider a perturbation of the (l, m) spherical harmonic for each variable. Namely we let $c(r, \phi) = c_0 + c_{l,m}(r)Y_{l,m}(\theta, \phi)e^{st}$ where c_0 is the homogeneous static solution given by $c_0 = k^{\text{off}}\mu_0/k^{\text{on}}$, and define along the same lines the other (l, m) components of the perturbation as $\psi_{l,m}, \delta\rho_{l,m}, \mu_{l,m}$. Solving Eq. (3) then gives $c_{l,m}(r) = \tilde{c}_{l,m}I_{l+1/2}(\sqrt{\frac{s}{D_c}}r)/\sqrt{r}$ in terms of the Bessel function I_n . We then obtain the following linearized homogeneous system:

$$s\delta\rho_{l,m} + k_d\delta\rho_{l,m} - \frac{l(l+1)}{R^2}\psi_{l,m} = 0 \quad (6)$$

$$-\zeta\mu_{l,m} - \alpha\delta\rho_{l,m} - \beta\frac{l(l+1)}{R^2}\delta\rho_{l,m} - \xi\psi_{l,m} = 0 \quad (7)$$

$$D_c \left((l+1 - k^{\text{on}}R/D_c)I_{l+1/2}(u) - uI_{l-1/2}(u) \right) \tilde{c}_{l,m} \quad (8)$$

$$+ k^{\text{off}}R^{3/2}\mu_{l,m} = 0$$

$$(s + k^{\text{off}} + \frac{l(l+1)}{R^2}D_\mu)\mu_{l,m} - \mu_0 \frac{l(l+1)}{R^2}\psi_{l,m} \quad (9)$$

$$-k^{\text{on}}\tilde{c}_{l,m}I_{l+1/2}(u)/\sqrt{R} = 0$$

where $u \equiv \sqrt{\frac{s}{D_c}}R$. Demanding a non zero solution yields an explicit equation for s which defines the dispersion relation of the problem. This equation, which is non polynomial, can be studied numerically and fully characterizes the linear dynamics of the problem. A simplified (and analytically tractable) dispersion relation can be obtained in the limit where curvature effects can be neglected, which essentially amounts to considering the equivalent 1D problem. This assumption is valid at time scales $\tau \gg R^2/D_c$, when the bulk concentration of myosin can be taken as constant. It can be shown that in this regime the dispersion relation is cubic in s and reads

$$\left((s + D_c k^2)(s + k^{\text{off}} + D_\mu k^2) + k^{\text{on}}(s + D_\mu k^2) \right) \times \left(\xi(s + k_d) + k^2(\alpha + \beta k^2) \right) + \zeta\mu_0 k^2 (s + k_d)(s + k^{\text{on}} + D_c k^2) = 0, \quad (10)$$

where $k^2 \equiv l(l+1)/R^2$. A numerical analysis shows that for the biologically relevant range of parameters (see figure 2), this 1D approximation is quantitatively very close to the exact dispersion relation, which means that in practice curvature effects can be neglected. This 1D approximation (10) is useful to determine the threshold activity beyond which the instability appears. Indeed, a straightforward analysis shows that beyond the critical value defined by

$$\zeta_c = -\frac{(D_c k^{\text{off}} + D_\mu k^{\text{on}})\xi}{\mu_0 k^{\text{on}}} \quad (11)$$

real positive solutions for s exist, which means that the homogeneous state is unstable and that cortical flows appear. This threshold is controlled by both the diffusion properties of myosin, which clearly stabilize the concentration profile, and the friction which governs the amplitude of the cortical flow. Importantly, this threshold is independent of the physical properties of the gel, α and β , which however enter in stabilizing terms determining the shape of the unstable pattern. Moreover, the analysis of Eq. (10) reveals that s is maximized for a finite mode l_{\max} which will be dominant to linear order and will characterize the developing flow pattern at least at short times. Figure (2) shows that the most unstable mode l_{\max} grows with the activity. Note that a full non linear treatment, which goes beyond the scope of this paper, would be necessary to discuss the long time behavior of the problem. Interestingly, the specific limit of fast exchange and fast depolymerization ($k^{\text{on}}, k^{\text{off}}, k_d$ large and $D_c = 0$ for simplicity) can be discussed at non linear order. In this case the dynamics takes the simplified form

$$\partial_t \mu = D_\mu \nabla^2 \mu + \frac{\zeta}{\xi} \nabla \cdot (\mu \nabla \mu), \quad (12)$$

which can be viewed as a modified Keller-Segel equation with drift $-\zeta/\xi \nabla \mu$ [16]. In this limit it can be shown that the solution blows-up as soon as $\mu > -\xi D_\mu / \zeta$. We expect that in the physical regime this singularity is damped leading to smoother asymptotic profiles.

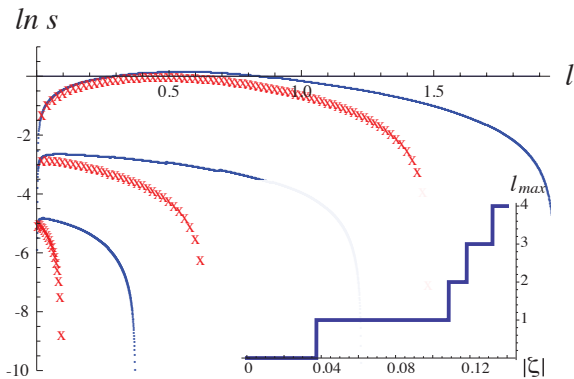


FIG. 2: Dispersion relation $s(l)$ in log scale: blue lines 1D (where $k = \sqrt{l(l+1)}/R$) and red crosses 3D. Pairs of curves in ascending order are for activities $\zeta = -0.01, -0.05, -0.1 \text{ kg } \mu\text{m s}^{-2}$. Inset : most unstable integer mode number l_{\max} (integer l when $s(l)$ is maximal), against the strength of activity $|\zeta|$. Other parameter values (order of magnitude estimates of biologically relevant values taken from [15, 17–22]): $k^{\text{on}} = 1 \mu\text{m s}^{-1}$, $k^{\text{off}} = 0.1 \text{ s}^{-1}$, $D_c = 10 \mu\text{m}^2 \text{ s}^{-1}$, $D_\mu = 1 \mu\text{m}^2 \text{ s}^{-1}$, $k_d = 0.1 \text{ s}^{-1}$, $\alpha = 1000 \text{ kg } \mu\text{m}^{-1} \text{ s}^{-2}$, $\beta = 1000 \text{ kg } \mu\text{m s}^{-2}$, $\xi = 0.1 \text{ kg } \mu\text{m}^{-3} \text{ s}^{-1}$, $R = 10 \mu\text{m}$ and $\mu_0 = 10^4 \mu\text{m}^{-2}$.

These results have several implications in the context of cell biology. Firstly, we show that such spontaneous cortical flows, which are observed in many contexts of cell

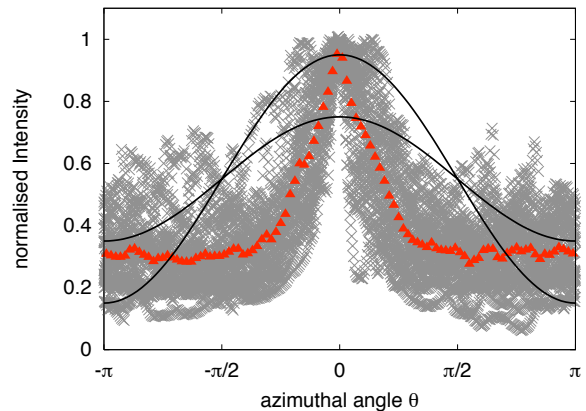


FIG. 3: Experimental data from [11] for the intensity of mCherry-Lifeact labeled actin around the cortex of MDA-MB-231 tumor cells seeded in 3D Matrigel. Theoretical line in black shows the predicted unstable mode $Y_{1,0}(\theta)$. Red triangles show the average of 19 individual cells shown with grey crosses. The position $\theta = 0$ is set at the maximum intensity along the perimeter and corresponds to the back of the moving cells.

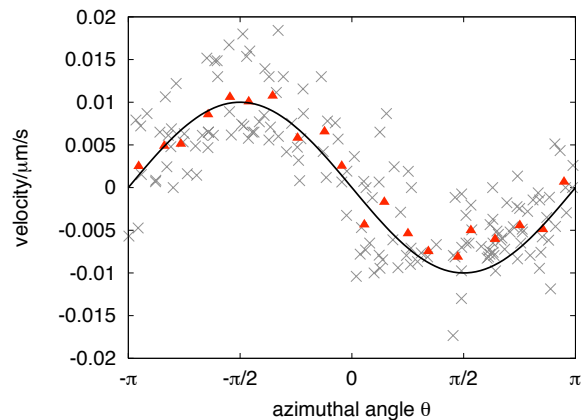


FIG. 4: Experimental data from [11] for the velocity of actin around the cell cortex calculated from kymographs (position over time) of the data in figure 3. Red triangles show the average of 9 individual cells shown with grey crosses. The same reference $\theta = 0$ as in figure 3 applies, with the black line showing the theoretical velocity of the predicted unstable mode $Y_{1,0}(\theta)$.

polarization and development [12, 13], can induce motion when the cell is embedded in a 3D medium. Quantitatively, the above analysis shows that for $\zeta > \zeta_c$ the mode $l = 1$, for which $\mu, \delta\rho, \psi$ are proportional to $Y_{1,0}(\theta)$, grows and creates a converging flow towards the pole $\theta = 0$ of the cell where the cortex thickens, while the pole $\theta = \pi$ depletes, as shown in figures (1,3,4). In fact, the friction law of Eq. (2) gives the tangential stress σ_{nt} on the sphere, which can be integrated to yield the force exerted by the medium on the cell in response to the spontaneous cortical flow. Assuming that the flow in the medium is

much slower than the cortical flow, this force is non zero and reads $F = \frac{8\pi}{3}h_0R^2\xi v_0$, where h_0 is the cortex thickness and v_0 is the amplitude of the cortical flow, showing that the instability of the mode $Y_{1,0}$ induces cell motion. Note that the flow produced in the medium in response to cell motion induces a friction force $-F$, so that globally the cell acts on the fluid as a force dipole as expected.

Secondly, we note that this cortical instability is closely related to bleb formation [14, 23–25]. In the unstable regime, we find that the cortex is weakened, and could even lead to a hole, for instance at the pole $\theta = \pi$ for the mode $Y_{1,0}(\theta)$. Above a certain activity threshold, the pressure inside the cell will be enough to break a weakened cortex, forming a bleb. Larger modes $l > 1$ correspond to several simultaneous blebs. Our proposed mechanism of bleb formation is closely related to that of [14], with the notable difference that their instabilities rely mainly on calcium dynamics.

Finally we compare these theoretical predictions to experiments conducted on MDA-MB-231 human breast adenocarcinoma cells seeded in 3D matrigel. These cells were found to invade and migrate in 3D matrigel with a striking round morphology, and to display neither membrane extension nor blebbing at the cell front, in contrast with classical experiments on flat substrates. Interestingly, silencing the main actin polymerization nucleator found in lamellipodial structures (Arp2/3) had no effect on the cell migration velocity, while it is known to be critical for migration on flat substrates. Moreover, inhibition of myosin II using blebbistatin almost completely abolished cell movement indicating that myosin activity is essential for movement. This shows that an alternative motility mechanism, widely independent of actin treadmilling and dependent on myosin contractility, must be involved to trigger migration. We suggest here that the cortical instability studied above, which relies mainly on cortical contractility could be the mechanism at work under these conditions. High resolution confocal imaging of live MDA-MB-231 cells in matrigel confirmed a highly non uniform distribution of cortical actin, which accumulates at the cell rear (see Fig.1 and [11]) in agreement with the model. More precisely, live imaging analysis of actin cortical structures indicated the quantity of cortical actin per perimeter length, quantified by ρ in the model. Figure (3) shows quantitatively the accumulation of actin at the back of the cell, and depletion at the front, in agreement with the predicted mode $Y_{1,0}$ which is unstable for $\zeta > \zeta_c$. Analysis of kymographs of these films provided the flow of cortical actin. Figure (4) shows that the velocity profile obtained is also compatible with the mode $Y_{1,0}$, which as we have shown induces cell motion. In addition, blocking beta1 integrin function with anti-human beta1 integrin monoclonal antibody 4B4 resulted in a strong reduction in migration and in the presence of blebs. In our model this corresponds to decreasing the friction parameter ξ and consequently the threshold

value ζ_c , which leads to a shift of the instability towards the higher modes $l > 1$, corresponding to the formation of multiple simultaneous blebs. Together these experiments [11] strongly suggest that in this example of cell migration in a 3D environment, motility is induced by the cortical instability described in the present paper.

To conclude, we have presented a generic model of cell motility generated by acto-myosin contraction of the cell cortex. We identified analytically dynamical instabilities and showed that spontaneous cortical flow can induce cell migration in 3D environments. Theoretical predictions compare well to experimental data of tumor cells migrating in 3D matrigel, and overall suggest that this contractility-based mechanism of spontaneous cortical flows generation could be a general mode of cell migration in 3D environments, which strongly differs from the classical picture of lamellipodial motility.

-
- [1] B. Alberts, *Molecular Biology of the cell* (Garland Science, New York, 2002), 4th ed.
 - [2] V. Noireaux et al., *Biophys. J.* **78**, 1643 (2000).
 - [3] A. Bernheim-Groswasser et al., *Nature* **417**, 308 (2002).
 - [4] F. J. Nedelec, T. Surrey, A. C. Maggs, and S. Leibler, *Nature* **389**, 305 (1997).
 - [5] K. Kruse et al., *Phys Rev Lett* **92**, 078101 (2004); *Eur Phys J E Soft Matter* **16**, 5 (2005).
 - [6] R. Voituriez, J. F. Joanny, and J. Prost, *Europhysics Letters* **70**, 404 (2005); *Phys Rev Lett* **96**, 028102 (2006); A. Zumdieck, R. Voituriez, J. Prost, and J. F. Joanny, *Faraday Discuss.* **139**, 369 (2008).
 - [7] D. Marenduzzo, E. Orlandini, M. E. Cates, and J. M. Yeomans, *Phys. Rev. E* **76**, 031921 (2007); *J. Non-Newton. Fluid Mech.* **149**, 56 (2008).
 - [8] P. T. Yam et al., *J. Cell Biol.* **178**, 1207 (2007).
 - [9] T. Lämmermann et al., et al., *Nature* **453**, 51 (2008).
 - [10] R. J. Hawkins et al., *Phys Rev Lett* **102**, 058103 (2009).
 - [11] R. Poincloux et al., submitted to PNAS (2010).
 - [12] D. Bray and J. White, *Science* **239**, 883 (1988).
 - [13] M. Mayer et al., *Nature* **467**, 617 (2010).
 - [14] G. Salbreux, J. F. Joanny, J. Prost, and P. Pullarkat, *Phys Biol* **4**, 268 (2007).
 - [15] A. C. Callan-Jones, J.-F. Joanny, and J. Prost, *Physical Review Letters* **100**, 258106 (2008).
 - [16] E. F. Keller and L. A. Segel, *J Theor Biol* **30**, 225 (1971).
 - [17] A. Mogilner and L. Edelstein-Keshet, *Biophys J* **83**, 1237 (2002).
 - [18] T. D. Pollard, L. Blanchoin, and R. D. Mullins, *Annu Rev Biophys Biomol Struct* **29**, 545 (2000).
 - [19] R. J. Hawkins, O. Bénichou, M. Piel, and R. Voituriez, *Phys Rev E* **80**, 040903 (2009).
 - [20] O. Wagner et al, *Biophys J* **76**, 2784 (1999).
 - [21] R. Niederman and T. D. Pollard, *J Cell Biol* **67**, 72 (1975).
 - [22] J. Kolega and D. L. Taylor, *Mol Biol Cell* **4**, 819 (1993).
 - [23] G. T. Charras et al., *Nature* **435**, 365 (2005).
 - [24] G. Charras and E. Paluch, *Nat Rev Mol Cell Biol* **9**, 730 (2008).
 - [25] J.-Y. Tinevez et al., *PNAS* **106**, 18581 (2009).